Induced currents in magnetic bearings: dynamical electromechanical model*

V. Kluyskens
CEREM
UCL
Louvain-la-Neuve, Belgium
kluyskens@prm.ucl.ac.be

B. Dehez
CEREM
UCL
Louvain-la-Neuve, Belgium
dehez@prm.ucl.ac.be

***Abstract*— Magnetic bearings are systems where strong interactions coexist between electro-magnetic and mechanical phenomenon. This paper presents an analysis of these interactions and of the way they can generate a potentially unstable behaviour. An analytical model is presented considering the electromagnetic nature of the forces and the general rotating machinery aspects. The coefficients of the model are found by identification with a finite element model of the system and with experimental measurements.**

***Index Terms*— Magnetic bearings, induced currents, dynamical instabilities model**

I. Introduction

Nowadays, magnetic bearings can be found in an increasing number of applications. Indeed, the contactless nature of these bearings destine them to be the ideal bearing in, among others, high-speed and vacuum applications.
Magnetic bearings can be classified as active, passive or semi-passive magnetic bearings. Semi-passive magnetic bearings combine the advantages of active and passive magnetic bearings. On one hand, they are less energy consuming and less costly than completely active magnetic bearings, and on the other hand they are controlled in some of their degrees of freedom, which allows the suspension to have positive stiffness in all directions.

These semi-passive magnetic bearings have already been tested and used notably in energy storage applications and in space applications. Generally, the stability study of a magnetic bearing is limited to the study of its static characteristics, and its gyroscopic effects [1], [2]. But when used in high-speed spinning systems, studies [3] have shown the onset of vibrations not predicted by a static and gyroscopic analysis: indeed they take place after critical speeds have been passed, and are not due to gyroscopic effects.
This paper presents the analysis of this observed potentially unstable dynamical behaviour of a rigid rotor supported by magnetic bearings. It shows how the unstable behaviour can be explained by the consideration of non-conservative forces, and the location where they take place.

*This work is supported by the Belgian Program for Inter-University Attraction Poles initiated by the Belgian State-Prime Minister's Office IAP-V-06.

In the first section of this paper, an analytical model is developed representing the behaviour of systems submitted to electromagnetic forces. These forces are represented by damping and spring coefficients, and by an electrical phase shift, resulting of the global resistance and the global inductance of the system.
In the second section, this analytical model is validated through a comparison with finite elements models of a simple electromagnetic case.
In the last section, the results of the finite element models of this simple case are compared with experimental results. Finally, it is concluded.

II. Electromechanical model

Magnetic bearings are electromechanical systems. From a mechanical point of view, their modelling is plainly related to general rotating machinery modelling but the forces acting between the rotor and the stator are of an electromagnetic nature.
This section will first show how the coupling of the rotational motion of the rotor and the dissipative nature of forces can generate an unstable behaviour. Talking about magnetic bearings, currents induced in the conducting parts of the rotor by the spinning of the rotor generate dissipative forces in the rotor. This leads us to the second part of this section where we adopt an electromechanical point of view to develop a model integrating the rotating modelling and the electromagnetic nature of the forces exerced on the rotor.

A. Mechanical equations

Let us write the equations of motion of a damped linear Jeffcott rotor. The Jeffcott rotor is a point mass, weighing m, attached to a massless shaft. The shaft produces an elastic restoring force of stiffness k on the rotor. The spin speed is ω. The damping in the system can be splitted in two:

- on one side, the damping taking place in the stator, called "non-rotating damping", and noted c_{nr} in the following sections,
- and on the other side, the damping taking place in the rotor, called "rotating damping", and noted c_r in

the following sections.

The position (x, y) of the rotor in the perpendicular to the rotation axis plane can be expressed by a complex vector $z = x + jy$. The equation of motion is, as explained in [4]:

$$m\ddot{z} + (c_{nr} + c_r)\dot{z} + (k - jc_r\omega)z = 0. \quad (1)$$

The solution $z = z_0 \exp(j\lambda t)$, with $\lambda = \lambda_R + \lambda_I j$ a complex number, corresponds to:

$$\begin{cases} x = z_0 \exp(-\lambda_I t)\cos(\lambda_R t) \\ y = z_0 \exp(-\lambda_I t)\sin(\lambda_R t) \end{cases}$$

It can be obtained for λ:

$$\lambda = \mp \frac{1}{\sqrt{2}}\sqrt{\Gamma + \sqrt{\Gamma^2 + (\omega c_r/m)^2}} + j\left(\frac{c_r + c_{nr}}{2m} \pm \frac{1}{\sqrt{2}}\sqrt{-\Gamma + \sqrt{\Gamma^2 + (\omega c_r/m)^2}}\right),$$

with:

$$\Gamma = \frac{k}{m} - \frac{(c_{nr} + c_r)^2}{4m^2}.$$

The first solution has a negative real part and an always positive imaginary part for λ: it corresponds to an always-damped backward whirl motion.
The second solution, corresponding to the positive real part of λ, represents a forward whirl motion. It is only damped when the imaginary part of λ is positive, that is for a spin speed ω smaller than the limit spin speed ω_{lim} given by:

$$\omega_{lim} = \sqrt{\frac{k}{m}}\left(1 + \frac{c_{nr}}{c_r}\right). \quad (2)$$

When $\omega > \omega_{lim}$, the forward whirl motion is permanently amplified.

It can here be observed that the rotating damping, which is a non-conservative force, has a destabilising role. When c_r is negligible in comparison to c_{nr}, the limit spin speed tends to infinity and there is no problem. But when c_r is not negligible, the behaviour of the rotor is unstable beyond a finite limit spin speed ω_{lim}. This limit spin speed is all the more smaller and tending to the critical speed $\sqrt{k/m}$ than the ratio c_{nr}/c_r is smaller.

B. Electromechanical model

In magnetic bearings, deliberate or not eddy currents can appear. Indeed, an electromotive force is induced in the conducting pieces of the magnetic bearing seeing a variable magnetic field because of an off-centred spinning motion of the rotor. This induced electromotive force produces currents in the conducting piece, which interact with the magnetic field to generate a Lorentz force.
From a mechanical modelling point of view, the electromagnetic forces acting on the system are represented by mechanical components like dampers or springs. The Lorentz force due to induced currents, being dissipative, can be represented by a damping coefficient. This damping coefficient will be c_r for induced currents taking place in the rotor, and will be c_{nr} for induced currents taking place in the stator.

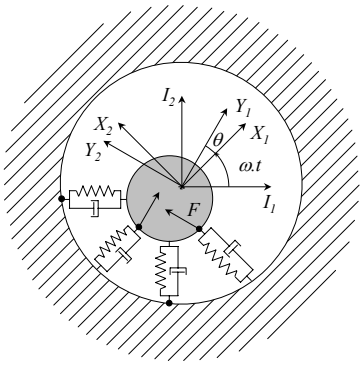

Fig. 1. schematic view of a rotor whirling within a stator, its corresponding frames and mechanical components to model the forces

Let's consider that the conducting piece where currents are induced has a global resistance R, and a global inductance is L. The electromotive force generates currents in the piece, with a phase shift of an angle $\theta = \arctan\frac{\omega L}{R}$. The interaction between the induced currents and the magnetic field creates an electromagnetic force perpendicular to the latter, so this force has the same phase shift.

The phase shift can be taken into account by introducing a phase shift in the forces modelled by a damper. For an only resistive piece, $\theta = 0$, the resultant force is perpendicular to the centre shift. On the other hand, for an only inductive piece, $\theta = \frac{\pi}{2}$, the resultant force is parallel to the centre shift.

We will consider in the following developments that there are induced currents only in the rotor. A first way to find the equation of motion, like explained in [5], is to work with a whirling frame attached to the rotor $\{\hat{X}\}$, and a second frame $\{\hat{Y}\}$ turning at the same speed as frame $\{\hat{X}\}$, but with a constant phase shift θ (Fig. 1). The force due to the induced currents is directed along the axis of frame $\{\hat{Y}\}$.

Another way to find the equation of motion is to introduce the notion of complex damping coefficient. Let us say that $c_r = c'_r + jc''_r$. The real part of c_r corresponds to the usual damping, whereas the imaginary part corresponds to a stiffness in the sense that it does not imply any energy dissipation.
Applied to induced currents, it can be noticed that

- c'_r represents the losses due to the resistance of the piece $c'_r = -c_r \cos\theta$
- c''_r represents the energy storage in the inductance of the piece $c''_r = c_r \sin\theta$

Finally, the equations of motion are in this case,

$$m\ddot{z} + (c_{nr} - c_r \cos\theta + j c_r \sin\theta)\dot{z} + (k + \omega c_r \sin\theta + j\omega c_r \cos\theta) z = 0. \quad (3)$$

It can be observed that in this case, there are non-diagonal terms not only in the stiffness matrix, but also in the damping matrix. The equation of motion can also be written:

$$\begin{pmatrix} m & 0 \\ 0 & m \end{pmatrix} \begin{pmatrix} \ddot{x}_I \\ \ddot{y}_I \end{pmatrix} = \begin{pmatrix} F_X \\ F_Y \end{pmatrix}, \quad (4)$$

with:

$$\begin{pmatrix} F_X \\ F_Y \end{pmatrix} = \begin{pmatrix} -c_{nr} + c_r \cos\theta & c_r \sin\theta \\ -c_r \sin\theta & -c_{nr} + c_r \cos\theta \end{pmatrix} \begin{pmatrix} \dot{x} \\ \dot{y} \end{pmatrix} + \begin{pmatrix} -k_{nr} - c_r\omega \sin\theta & c_r\omega \cos\theta \\ -c_r\omega \cos\theta & -k_{nr} - c_r\omega \sin\theta \end{pmatrix} \begin{pmatrix} x \\ y \end{pmatrix}. \quad (5)$$

Stability conditions becomes in this case:

$$\boxed{\omega_{lim} = (1 + \frac{c_{nr}}{c_r \cos\theta})(w_{dyn} \pm \sqrt{\omega_{dyn}^2 + \omega_{cr}^2})} \quad (6)$$

with

$$\omega_{cr} = \sqrt{k/m}$$
$$\omega_{dyn} = c_{nr} \tan\theta/(2m)$$

Eq. (6) is non linear and has to be solved by iterations. With no phase shift ($\theta = 0$, only resistive piece) we find the previous stability condition again (2).
When θ grows, i.e. the inductance of the piece is not zero, the limit speed gets bigger and is less restrictive.
When θ tends to $\frac{\pi}{2}$ (only inductive piece), the limit speed tends to infinity, and the system tends to become unconditionally stable. This is the case of supraconductors: the resistance is almost zero, and the system is unconditionally stable.

III. Finite elements validation

To validate this model, the electromechanical model is confronted to a case study modelled by a finite element modelling software.

The simple case chosen for this comparison is an aluminium disk (diameter 60 mm, height 10 mm) spinning in a vertical magnetic field, as shown in Fig. 2. The two permanent magnets used to generate this magnetic field are charcterized by a magnetisation directed parallel to the rotation axis, and by a residual induction is worth 1.21T. Their dimensions are 5x10x40 mm. The centre of rotation of the disk lay away from the permanent magnets with a distance d. The disk has a height of 10 mm, and the air gap between the magnets and the disk is 1 mm.

A. Parameter identification

In the analytical model, different parameters are unknown. First, they will be determined by interpreting the physical phenomenon involved, and afterwards the remaining parameters will be found by identification between the analytical expression of the forces and the estimation of the forces by a finite elements model.

Analysing the study case, it can be observed that:

- $k = 0$, and $c_{nr} = 0$.

Indeed, when the ring is not moving ($\omega = 0$), no forces are exerced on it (aluminium is not ferromagnetic). This means that the stiffness k is worth zero. Furthermore, when the conducting piece is moving, there are no losses in the non-rotating magnets ($c_{nr} = 0$).
It can be noted that this particular system is always unstable! ($\omega_{lim} = 0$, see (6)).
Moreover, in this study case, $x = d$, $y = 0$, $\dot{x} = 0$ and $\dot{y} = 0$ in (5): the centre of the ring is fixed.

$$F_X = -c_r\omega \sin\theta d, \quad (7)$$
$$F_Y = -c_r\omega \cos\theta d. \quad (8)$$

The two left parameters are c_r and θ.

The first way to identify them is to apply the least square criterion to the forces resulting from the model ((7) and (8)) and the forces calculated by the finite elements method.
Another way to identify c_r and θ is to use the ratio between (7) and (8), we get

$$F_X/F_Y = \tan\theta = \omega L/R \quad (9)$$

The ratio L/R is identified using the least square criterion. To find c_r, the rotation speed of the disk is set to zero, and the disk is given a vertical speed: $x = d$, $\omega = 0$ and $\dot{y} = v$.

$$F_X = 0, \quad (10)$$
$$F_Y = c_r v. \quad (11)$$

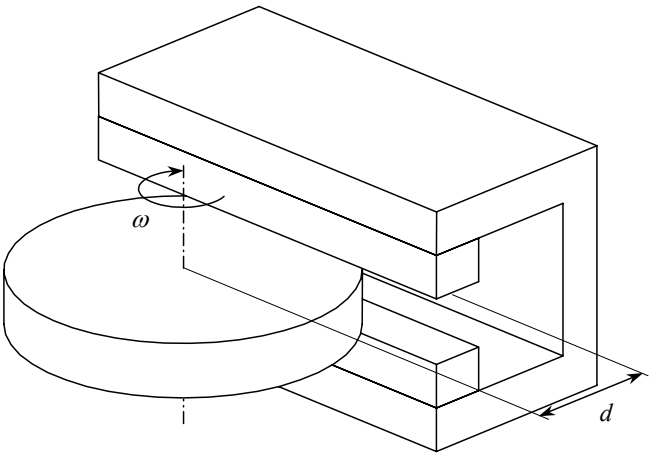

Fig. 2. Assembly chosen to validate model: aluminium disk rotating in a vertical magnetic field

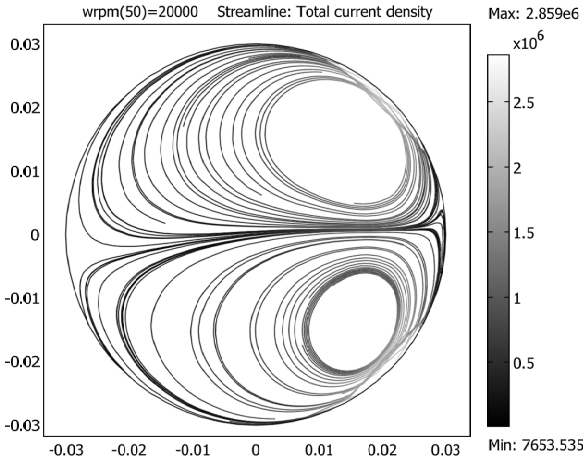

Fig. 3. induced currents in an aluminium ring rotating at 10000 rpm

Again, the parameter c_r can be identified with the least square criterion.

B. Two dimension finite elements model

We performed a first identification on the basis of a 2D FE model.
In this cas, it is supposed that the magnetic field generated by the permanent magnet in Fig. 2 is not function of z within the disk. This means that any slice of the disk sees the same magnetic field and we can make a 2D model of the assembly. On Fig. 3, the shape of the induced currents can be observed. Those currents interact with the magnetic field to generate a force directed along the x-axis F_x, and a force directed along the y-axis F_y.

For $d = 25mm$ using the first identification method((7) and (8)), it can be found for those parameters:

- $c_r = 0.0297$ Ns/m,
- $\theta = \arctan \frac{\omega L}{R} = \arctan(\omega\ 0.00183)$,

The results are shown on Fig. 4 and 5.
Using the second identification method ((9) and (8)), the values found for c_r and θ are:

- $c_r = 0.0217$ Ns/m,
- $\theta = \arctan \frac{\omega L}{R} = \arctan(\omega\ 0.00183)$.

First, it can be noticed that the results found for the two parameters are very close, and either of the two methods can be used. The advantage of the first method is that only one FE model has to be solved. The advantage of the second method is that each parameter is found separately, which simplifies the identification.
Second, it can be observed that the evolution predicted by the analytical model corresponds quite approximately to the evolution predicted by the finite elements model.
Let us note however that the validation was carried out on a 3D structure degenerated into a 2D structure neglecting among others the magnetic field penetration depth in the disk.

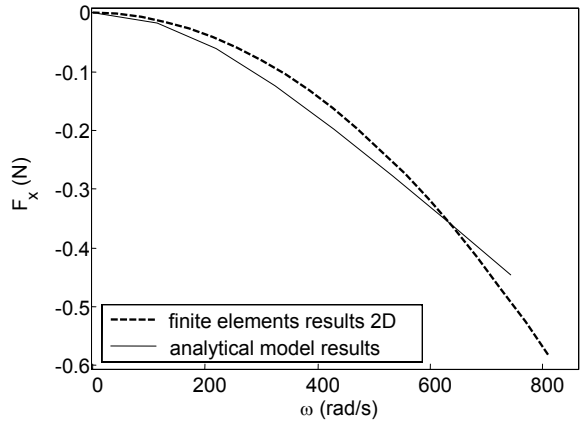

Fig. 4. F_x: Comparison between model force and 2D finite elements results

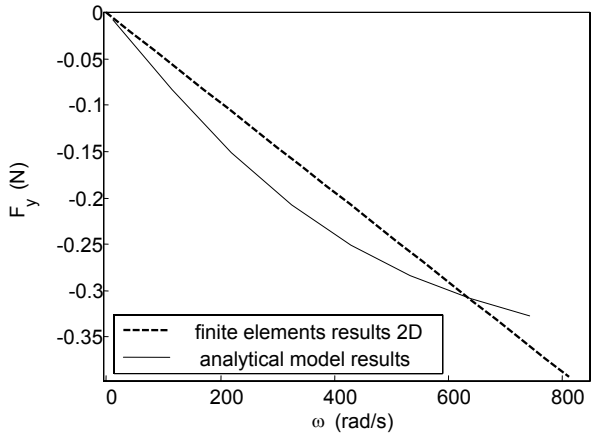

Fig. 5. F_y: Comparison between model force and 2D finite elements results

C. Three dimension finite elements model

To complete this 2D study, we performed a second identification on the basis of a 3D FE model.
For this 3D model, it can be noted that the system includes a plane of symmetry, so only half of the model has to be solved (see Fig. 6).

Again, the parameters of the analytical model are found by applying the least square criterion on the forces calculated by the FE model and the parameterised analytical model forces.
It is found

- $c_r = 0.733$ Ns/m,

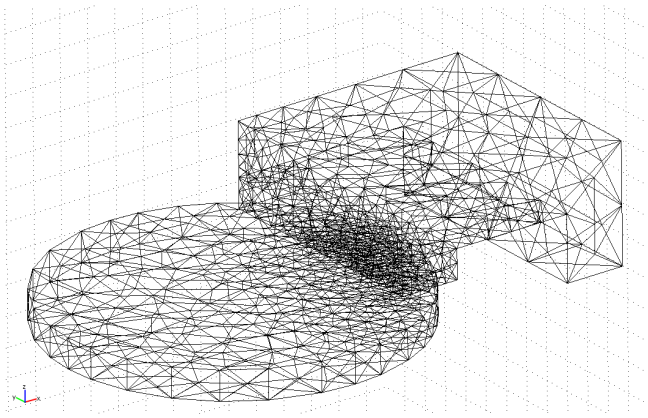

Fig. 6. Meshed model for finite elements modelling

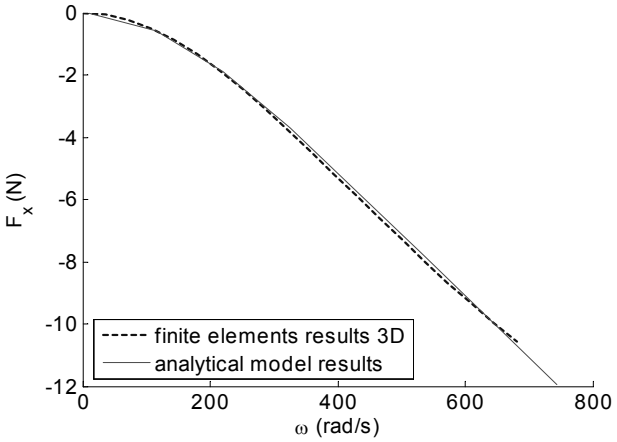

Fig. 7. F_x: Comparison between model force and 3D finite elements results

- $\theta = \arctan \frac{\omega L}{R} = \arctan(\omega\ 0.00244)$.

It can be seen on Fig. 7 and Fig. 8 that the forces predicted by the analytical and 3D FE models match.
Besides, it can also be seen that the forces predicted by the 3D FE model are much bigger than the forces predicted by the 2D FE model.

IV. Experimental validation

The difference between the forces predicted by the 2D and 3D FE model of the system is substantial.
In order to decide between the two FE models, we have completed our study by an experimental validation.

The experimental set up of the system is the following (see Fig.9): the aluminium disk is driven by a milling machine allowing rotation speeds up to 6300 rpm. Through the action-reaction principle, the forces exerced by the magnetic circuit on the disk are opposed to the forces exerced by the disk on the magnetic circuit. We measure the latter by a force/torque sensor attached to the magnetic circuit.

The results are shown on Fig. 10 and Fig. 11. The experimental measurements and the predicted forces by the 3D FE model correspond to each other. The small differences observed are probably due to the heating of the aluminium disk via the induced currents, influencing its resistivity, to measurement uncertainties, and to FE calculation inaccuracies.
On Fig. 10 and Fig. 11, the results of the analytical model are also shown. In this case, the parameter identifications has been done on the basis of the experimental measured forces. This gives:

- $c_r = 0.7176$ Ns/m (97.9% of c_r found via 3D FE model),
- $\theta = \arctan \frac{\omega L}{R} = \arctan(\omega\ 0.0032)$ (132% of $\frac{L}{R}$ found via 3D FE model).

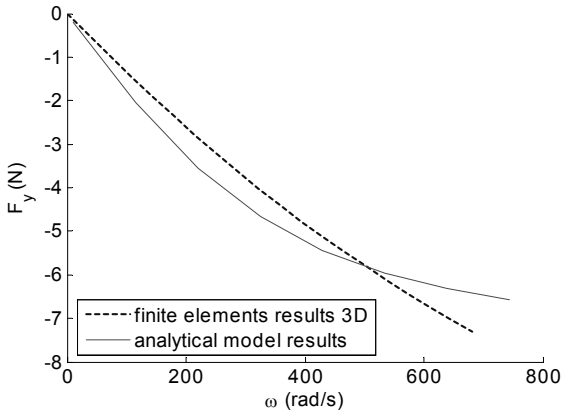

Fig. 8. F_y: Comparison between model force and 3D finite elements results

It can be said that either of the FE model or of the experimental results can be used to identify to analytical model parameters.

Lastly, it is interesting to observe the evolution of the parameters c_r and $\theta = atan(\omega L/R)$ with the distance d. Table I shows the evolution of damping and phase shift with distance d. At this stage, it seems difficult to find an analytical law to predict this evolution.

TABLE I
Evolution of c_r and θ with d

d (mm)	25	24	23	22	21	20
c_r(Ns/m)	0.733	0.829	0.951	1.0325	1.1559	1.216
L/R (mH/Ω)	2.44e	1.99	1.45	1.25	0.811	0.623

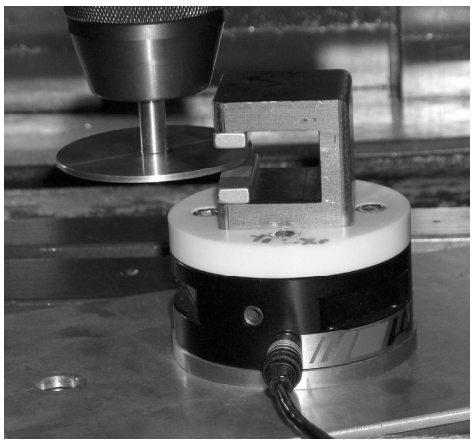

Fig. 9. Experimental set up to measure forces

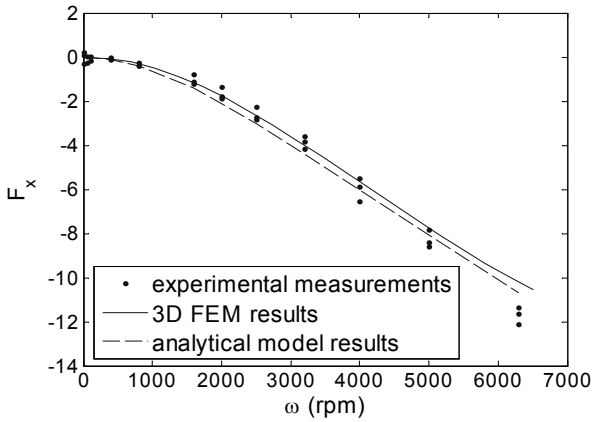

Fig. 10. F_x: Comparison between experimental measured forces, finite elements predicted forces and electromechanical model

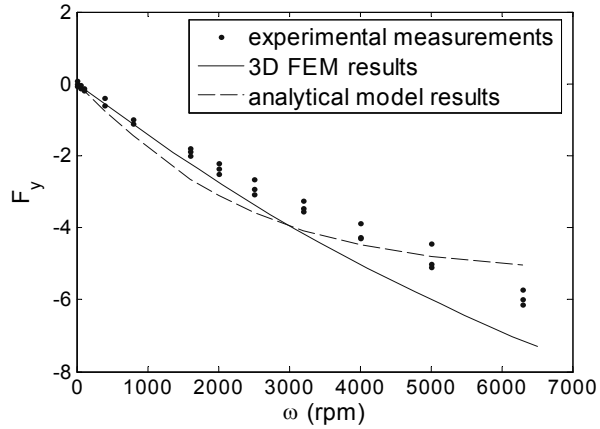

Fig. 11. F_y: Comparison between experimental measured forces, finite elements predicted forces and electromechanical model

V. Conclusion

An analytical model has been presented representing the behaviour of systems submitted to electromagnetic forces. These forces were represented by mechanical components as damping and spring coefficients, and by an electrical phase shift. The comparison of the evolution of the forces between FE and analytical models is convincing. The results of the 3D FE model also corresponds to the experimental results.

The parameters of this model are easily identified using finite elements or experimental results, but since it is difficult to characterize their evolution with the position of the rotor via a single evolution law, they should be identified point by point.

It can be concluded that the electromechanical model and the assumptions introduced to obtain it are valid. In particular, the idea of characterizing the rotating part by a resistance global R and an inductance global L seems correct.

In the long term, the electromechanical model presented in this paper, completely identified via FE modelling or experiments, should allow us to predict the dynamical behaviour of semi-passive magnetic bearings subject to important eddy current losses in the rotating part. To increase the stability of the system, appropriate changes can be made to its intrinsic parameters. The stability can be increased by working on the rotor (i.e. rotating damping c_r and ratio $\frac{L}{R}$), by working on the stator (non-rotating damping c_{nr}), or by having recourse to an external damping system, taking place between the stator and the inertial base. The electromechanical model presented in this article gives us a practical tool to analyse and understand the behaviour of the modified system before implementing these different solutions.

References

[1] G. Schweitzer, H. Bleuler, A. Traxley, "Active magnetic bearings: basics, properties and applications of active magnetic bearings," Vdf. Zurich, ISBN 3728121320

[2] J. Delamare, "Partially passive magnetic suspensions,"(in French), PhD. thesis, INP Grenoble, 1994

[3] F. Faure, "Magnetic suspension for flying wheel,"(in French), PhD. thesis, INP Grenoble, 2003

[4] G. Genta, "Vibration of structures and machines: practical aspects,"third edition, Springer, 1999, ISBN 0387985069

[5] V. Kluyskens, B. Dehez, H. Ben Ahmed, "Dynamical electromechanical model for passive bearings," unpublished